Fractal Structure of Nature's Preferred Masses: Application of the Model of Oscillations in a Chain System

Andreas Ries and Marcus Vinicius Lia Fook

Universidade Federal de Campina Grande, Unidade Acadêmica de Engenharia de Materiais, Rua Aprígio Veloso 882, 58429-140 Campina Grande — PB, Brazil
E-mail: andreasries@yahoo.com, marcusvinicius@dema.ufcg.edu.br

A numerical analysis of elementary particle masses on the logarithmic number line revealed systematic mass gaps of $2e$, e, $\frac{e}{2}$, $\frac{e}{4}$, $\frac{e}{8}$ and $\frac{e}{16}$. Also in abundance data of the chemical elements, a repeated abundance gap of $\frac{e}{2}$ could be detected. This lead us to modify a fractal scaling model originally published by Müller in this journal, interpreting elementary particles as proton resonances. We express a set of 78 accurately determined particle masses on the logarithmic scale in a continued fraction form where all numerators are Euler's number.

1 Introduction

Recently in three papers of this journal, Müller [1–3] has proposed a chain of similar harmonic oscillators as a new model to describe the fractal properties of nature. For a specific process or data set, this model treats observables such as energies, frequencies, lengths and masses as resonance oscillation modes and aims at predicting naturally preferred values for these parameters. The starting point of the model is the fact that hydrogen is the most abundant element in the universe and therefore the dominant oscillation state. Consequently, Müller calculates the spectrum of eigenfrequencies of a chain system of many proton harmonic oscillators according to a continued fraction equation [2]

$$f = f_p \exp S \,, \tag{1}$$

where f is any natural oscillation frequency of the chain system, f_p the oscillation frequency of one proton and S the continued fraction corresponding to f. S was suggested to be in the canonical form with all partial numerators equal 1 and the partial denominators are positive or negative integer values

$$S = n_0 + \cfrac{1}{n_1 + \cfrac{1}{n_2 + \cfrac{1}{n_3 + \ldots}}} \,. \tag{2}$$

Particularly interesting properties arise when the nominator equals 2 and all denominators are divisible by 3. Such fractions divide the logarithmic scale in allowed values and empty gaps, i.e. ranges of numbers which cannot be expressed with this type of continued fractions. He showed that these continuous fractions generate a self-similar and discrete spectrum of eigenvalues [1], that is also logarithmically invariant. Maximum spectral density areas arise when the free link n_0 and the partial denominators n_i are divisible by 3.

This model was applied to the mass distribution of celestial bodies in our solar system [2] as well as to the mass distribution of elementary particles such as baryons, mesons, leptons and gauge bosons [3]. The masses were found to be located at or close to spectral nodes and definitively not random.

In this article we investigated the properties of masses in the micro-cosmos on the logarithmic scale by a graphical analysis with particular interest in detection of periodic trends. We analyzed abundance data of the chemical elements, atomic masses and the masses of elementary particles. Then we applied a slightly modified version of Müller's fractal model and demonstrate that there is a hidden structure in the masses of elementary particles.

2 Data sources and computational details

Solar system abundance data of chemical elements (with uncertainties of around 10%) were taken from reference [4]. High accuracy nuclide masses are given in an evaluation by Audi [5]. Relative isotope abundances for a selected chemical element can be found in the CRC Handbook of Chemistry and Physics [6]. Accurate masses of elementary particles are given in Müller's article [3] and were used for the calculation of continued fractions. In order to avoid machine based rounding errors, numerical values of continued fractions were always calculated using the the Lenz algorithm as indicated in reference [7].

3 Results

Figure 1 shows the relative abundance of the chemical elements in a less usual form. In textbooks or articles these data are normally presented as $log_{10}(abundance)$ versus atomic number on a linear scale. Here we adopted Müller's formalism and present the abundance data as a function of the natural logarithm of the atomic masses (here mean values from a periodic table were used) which were previously divided by the lowest atomic weight available (hydrogen). As can be seen, there is a general trend of decreasing abundance with increasing atomic mass, but the plot has a few remarkable extremities.

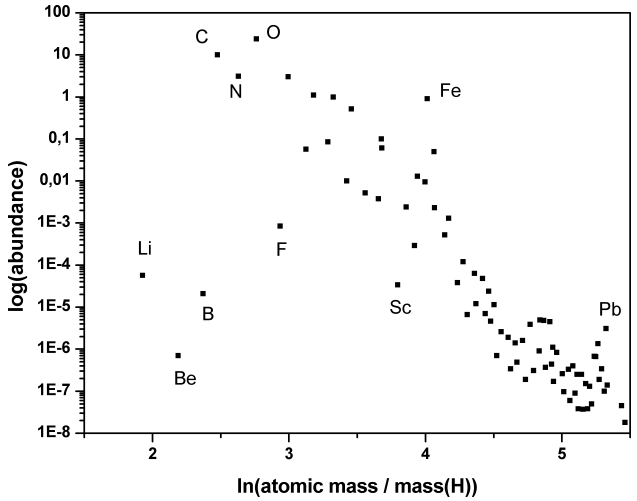

Fig. 1: Solar system abundance data of the chemical elements on a logarithmic scale. H and He omitted for clarity.

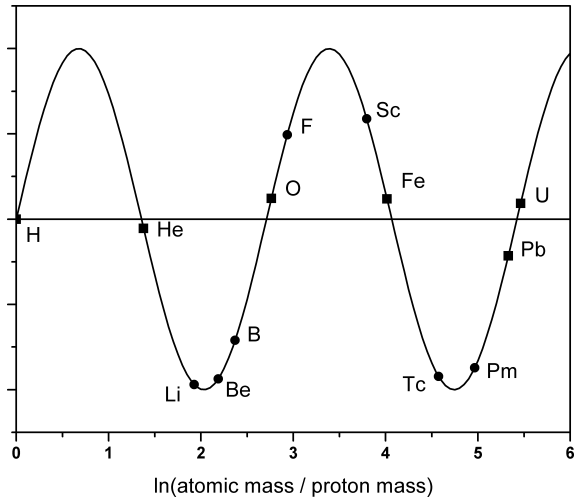

Fig. 2: Abundance maxima and minima of chemical elements on the logarithmic number line.

Nuclide	$\ln \frac{m(nuclide)}{m(\mathrm{H})}$	multiples of $\frac{e}{2}$
$^{1}_{1}$H	0.0	$0.0 \times \frac{e}{2}$
$^{4}_{2}$He	1.379	$1.015 \times \frac{e}{2}$
$^{16}_{8}$O	2.764	$2.034 \times \frac{e}{2}$
$^{56}_{26}$Fe	4.016	$2.955 \times \frac{e}{2}$
$^{208}_{82}$Pb	5.330	$3.921 \times \frac{e}{2}$

Table 1: $\ln \frac{m(nuclide)}{m(\mathrm{H})}$ of element abundance maxima expressed in multiples of $\frac{e}{2}$.

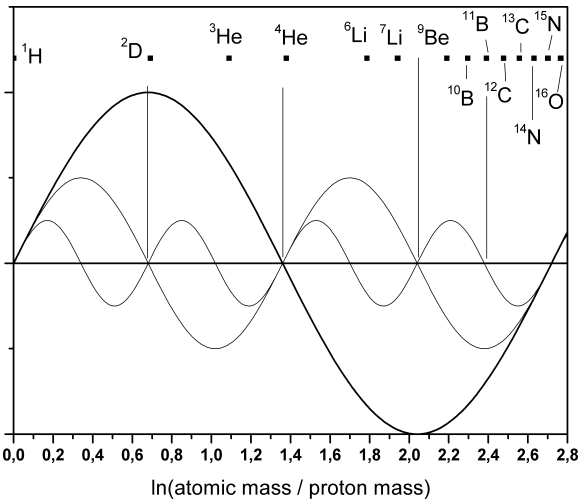

Fig. 3: Stable isotopes on the logarithmic scale in the range 0 to e.

Elements marking very clear maxima or minima are labeled with symbols. The most relevant maxima in graph are elements O, Fe and Pb. Of course, H and He, the most abundant elements in the universe (not shown in Fig. 1) must also be interpreted as maxima in the figure. From Figure 2 it becomes directly clear that these abundance maxima occur in almost equal distances on the logarithmic number line. The simple calculation $\ln \frac{m(^4_2\mathrm{He})}{m(^1_1\mathrm{H})} - \ln \frac{m(^1_1\mathrm{H})}{m(^1_1\mathrm{H})} = 1.37$ reveals that these distance seems to be $\frac{e}{2}$, where e is Euler's number. When drawing a sine function with period e, $f(x) = \sin(\frac{2\pi x}{e})$ on the logarithmic number line, the abundance maxima are closely located to the zeros of this function.

Table 1 summarizes the numerical deviations from multiples of $\frac{e}{2}$. The calculations were performed for the naturally most abundant isotope of the considered element.

Figure 2 has some analogy to Kundt's famous experiment with standing sound waves in a tube. It seems as a standing wave on the logarithmic number line supporting an accumulation of naturally preferred mass particles in the nodes, which are multiples of $\frac{e}{2}$. On the other hand these preferred masses are not exactly located in the notes, more evidently the less abundant chemical elements (Li, Be, B, F) are more distant from the bulges than H, He, O, Fe and U from the nodes. Pm and Tc are even completely absent in the abundance data due to their radioactivity.

Within the first period of the sine function in Fig. 2, very few stable isotopes are found. So it is possible to analyze the location of their isotope masses in relation to nodes of the previously constructed sine function including higher harmonics. Figure 3 displays the logarithmic axis from zero to e with a sine function of period e and two corresponding (2nd and 4th) higher harmonics defined through repeated frequency doubling. The location ($= \ln \frac{m_{nuclide}}{m_{proton}}$) of all existing stable isotopes in that range is indicated. From this, similar wave stabilizations regarding these light isotopes can be obtained:

1. Deuterium is a stable, but hardly abundant hydrogen isotope. It seems to be stabilized by the second harmonics with period $\frac{e}{2}$ due to location in the node (tritium does not fit in a node of this wave). Possibly hy-

drogen isotopes are principally governed by the basic wave with period e and the influence of higher harmonics is greatly reduced, which explains the low abundance.

2. Why is the isotope ^{4}He (99.999%) much more abundant than ^{3}He (0.0001%)? Assuming that He is principally governed as H by the wave with period e, the isotope ^{4}He is closer to the node than ^{3}He. In this case the higher stability of ^{4}He can also explained with the magic numbers for both, protons and neutrons.
3. Lithium is composed of 92.5% ^{7}Li and 7.5% ^{6}Li. The isotope ^{7}Li is more abundant and clearly closer to a node of the second harmonic (it has also a little higher bonding energy per nucleon than ^{6}Li).
4. The isotope ^{11}B is exactly located in the node of the third harmonic with period $\frac{e}{4}$. It is much more abundant (80.1%) than ^{10}B (19.9%).
5. The isotope ^{12}C is closer to the node of the fourth harmonics than ^{13}C. This is in agreement with the abundances of 98.0% for ^{12}C and 1.1% for ^{13}C.
6. Nitrogen is composed of 99.63% ^{14}N and 0.36% ^{15}N. The isotope ^{15}N is almost in the node of the basic wave and all higher harmonics. Here the model fails to predict the correct abundance order, but the isotope ^{15}N has the higher stability, which can be readily confirmed by the magic number of 8 neutrons in this nuclide. For a certain reason, the nuclide stability does not go along with the corresponding abundance. For an explanation of this fact must be considered that elements heavier than He cannot be built up in our sun or similar present-day (second generation) stars [8]. This is due to the fact that for all nuclei lighter than carbon, a nuclear reaction with a proton leads to the emission of an alpha particle disintegrating the original nucleus. So the heavier elements in stars must already have existed prior to the second generation star formation. Bethe [8] investigated possible nuclear reactions of both nitrogen isotopes and found that ^{15}N can give a $p-\alpha$ reaction

$$^{15}\mathrm{N} + {}^{1}\mathrm{H} \rightarrow {}^{4}\mathrm{He} + {}^{12}\mathrm{C}$$

while ^{14}N can only capture a proton

$$^{14}\mathrm{N} + {}^{1}\mathrm{H} \rightarrow {}^{15}\mathrm{O} + \gamma.$$

According to Bethe, such a $p-\alpha$ reaction is always more probable than a radiative capture. So we theorize that without existence of the above mentioned nuclear reaction, the abundance data would show an excess of ^{15}N.

A nuclear reaction also explains why lead is the element with the highest deviation from such a node (Fig. 2). We believe that Pb does actually not present its true abundance value as existed through stellar element formation, its abundance is increased since it is the end product of the 3 most important decay chains (thorium series, uranium series, actinium series). There are no stable isotopes between Pb and ^{238}U, which has a long half-life. The element uranium lies much more close to a node than Pb, and also because of its long half-life, we believe that this nuclide could be a former abundance maximum.

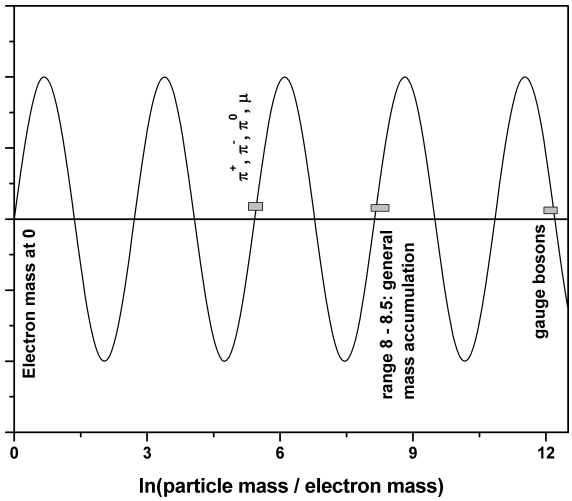

Fig. 4: Accumulation of particle masses on the logarithmic scale.

In order to find similar regularities for elementary particles we selected according to some physics textbooks a set of commonly discussed particles. Their importance was mainly justified by the relatively long lifetimes ($> 10^{-19}$ s). We believe that nature's preferred masses are the more stable particles and particularly for these masses some regularities could be expected. Table 2 presents the considered set of particles, their rest masses and positions on the logarithmic scale. It was found that the particles produce an interesting set of mass distances on the logarithmic number line: $2e$, e, $\frac{e}{2}$, $\frac{e}{4}$, $\frac{e}{8}$ and $\frac{e}{16}$. These mass gaps are listed in Table 3. There is, however, no standing wave analogy on the logarithmic scale that can be applied to all particles, consequently here, another model must be applied, which lead us to modify Müller's continued fraction term in an empirical way. However, the standing wave analogy is not completely absent. Müller [3] has shown that the majority of baryon and meson masses is in the range of 1300–8600 MeV/c^2. When scaling according to $\ln \frac{m_{particle}}{m_{electron}}$, this range translates to 8–8.5 on the logarithmic scale and it becomes clear that this range and as well as the masses of the electron, muon, pion and gauge bosons are in proximity of the zeros of the above considered sine function (see Figure 4).

Considering the framework of Müller's fractal scaling model, we interpret these numerical regularities as follows: Masses in nature are in relation to proton resonance states. Nature can realize various masses, only when they are close to proton resonance states, they are preferred masses. For stable particles such as nuclides, the term "preferred mass" translates to more abundance. For unstable particles, "preferred mass" translates to more realization probability. Un-

Particle	Rest mass m [MeV/c^2]	$\ln \frac{m(particle)}{m(proton)}$
Leptons:		
Electron	0.511	−7.515
μ	105.658	−2.183
τ	1776.84	0.638
Mesons:		
$\pi^{\pm}$	139.57	−1.905
π^0	134.9766	−1.939
$K^{\pm}$	493.677	−0.642
K^0_S, K^0_L	497.614	−0.634
η	547.853	−0.538
$\rho^{\pm}$	770	−0.198
ρ^0	775.5	−0.191
ω	782.6	−0.181
η^0	957.8	0.021
$K^{*\pm}$	891.7	−0.051
K^{*0}	896.0	−0.046
ϕ	1019.5	0.083
$D^{\pm}, D^0$	1869.6	0.689
$D^{\pm}_s$	1968.5	0.741
J/Ψ	3096.9	1.194
$B^{\pm}, B^0$	5279.2	1.727
Y	9460.3	2.311
Baryons:		
p	938.272	0
n	939.56	0.001
Λ^0	1115.6	0.173
Σ^+	1189.4	0.237
Σ^0	1192.5	0.240
Σ^-	1197.3	0.244
$\Delta^{\pm}, \Delta^{++}, \Delta^0$	1232	0.272
Ξ^0	1314.9	0.337
Ξ^-	1321.3	0.342
Ω	1672	0.578
Λ^+_C	2281	0.888
Λ^0_b	5624	1.791
Ξ_b	5774	1.817
Ξ^{-*}, Ξ^{0*}	15300	2.792

Table 2: Selected particles with rest masses and values on the logarithmic number line.

Particle mass step	Rest mass difference on logarithmic scale	Numerical result
Mass gap 2*e* (= 5.436):		
Electron → μ	$\lvert -7.515 - -2.183\rvert$	5.332
Mass gap *e* (= 2.718):		
$p \to \Xi^{-*}, \Xi^{0*}$	$\lvert 0 - 2.792\rvert$	2.792
Mass gap $\frac{e}{2}$ (= 1.359):		
$\pi^0 \to K^{\pm}$	$\lvert -1.939 - -0.642\rvert$	1.297
$\Xi^0 \to B^{\pm}, B^0$	$\lvert 0.337 - 1.727\rvert$	1.390
$\Lambda^+_C \to Y$	$\lvert 0.888 - 2.311\rvert$	1.423
Mass gap $\frac{e}{4}$ (= 0.68):		
$K^0_S, K^0_L \to p$	$\lvert -0.634 - 0\rvert$	0.634
$\Lambda^0 \to \Lambda^+_C$	$\lvert 0.173 - 0.888\rvert$	0.715
$p \to D^{\pm}, D^0$	$\lvert 0 - 0.689\rvert$	0.689
$p \to D^{\pm}_s$	$\lvert 0 - 0.741\rvert$	0.741
$p \to \tau$	$\lvert 0 - 0.638\rvert$	0.638
Mass gap $\frac{e}{8}$ (= 0.34):		
$\eta \to \rho^{\pm}$	$\lvert -0.538 - -0.198\rvert$	0.340
$p \to \Xi^0$	$\lvert 0 - 0.337\rvert$	0.337
$p \to \Xi^-$	$\lvert 0 - 0.342\rvert$	0.342
$\eta \to \rho^0$	$\lvert -0.538 - -0.191\rvert$	0.347
$\eta \to \rho^{\pm}$	$\lvert -0.538 - -0.198\rvert$	0.340
$\Sigma^+ \to \Omega$	$\lvert 0.237 - 0.578\rvert$	0.341
$\Sigma^0 \to \Omega$	$\lvert 0.240 - 0.578\rvert$	0.338
$\Sigma^- \to \Omega$	$\lvert 0.244 - 0.578\rvert$	0.334
$\Lambda^+_C \to J/\Psi$	$\lvert 0.888 - 1.194\rvert$	0.306
$\Omega \to \Lambda^+_C$	$\lvert 0.578 - 0.888\rvert$	0.310
Mass gap $\frac{e}{16}$ (= 0.17):		
$\omega \to p$	$\lvert -0.181 - 0\rvert$	0.181
$\rho^{\pm} \to p$	$\lvert -0.198 - 0\rvert$	0.198
$\rho^0 \to p$	$\lvert -0.191 - 0\rvert$	0.191
$p \to \Lambda^0$	$\lvert 0 - 0.173\rvert$	0.173
$\Lambda^0 \to \Xi^0$	$\lvert 0.173 - 0.337\rvert$	0.164
$\Lambda^0 \to \Xi^-$	$\lvert 0.173 - 0.342\rvert$	0.169
$\Omega \to D^{\pm}_s$	$\lvert 0.578 - 0.741\rvert$	0.163
$D^{\pm}_s \to \Lambda^+_C$	$\lvert 0.741 - 0.888\rvert$	0.147
$D^{\pm}, D^0 \to \Lambda^+_C$	$\lvert 0.689 - 0.888\rvert$	0.199

Table 3: Mass gaps between elementary particles on the logarithmic scale.

Particle	Particle mass with standard deviation. Continued fraction representation
N-baryons (S=0, I=1/2):	
p	938.27203 ±0.00008 [0; 0]
n	939.565346 ±0.000023 [0; 0 | 1973]
Λ-baryons (S=−1, I=0):	
Λ	1115.683 ±0.006 [0; 0 | 15, $e+1$, 15, −6]
$\Lambda(1520)$	1519.5 ±1.0 [0; 0 | 6, −9, $e+1$, $-e-1$, ***]
Σ-baryons (S=−1, I=1):	
Σ^+	1189.37 ±0.07 [0; 0 | 12, −6, $e+1$, $-e-1$, 6]
Σ^0	1192.642 ±0.024 [0; 0 | 12, $-e-1$, −9, $e+1$, $-e-1$, ***]
Σ^-	1197.449 ±0.03 [0; 0 | 12, $-e-1$, 6, $-e-1$, $e+1$, $-e-1$]
$\Sigma(1385)^+$	1382.8 ±0.4 [0; 0 | 6, $e+1$, $-e-1$, ***]
$\Sigma(1385)^0$	1383.7 ±1.0 [0; 0 | 6, $e+1$, $-e-1$, $e+1$, $-e-1$]
$\Sigma(1385)^-$	1387.2 ±0.5 [0; 0 | 6, $e+1$, $-e-1$, $e+1$, $e+1$]
Ξ-baryons (S=−2, I=1/2):	
Ξ^0	1314.86 ±0.2 [0; 0 | 9, $-e-1$, $e+1$, −6]
Ξ^-	1321.71 ±0.07 [0; 0 | 9, $-e-1$, $e+1$, ***]
$\Xi(1530)^0$	1531.8 ±0.32 [0; 0 | 6, −6]
$\Xi(1530)^-$	1535.0 ±0.6 [0; 0 | 6, −6, 9]
Ω-baryons (S=−3, I=0):	
Ω^-	1672.45 ±0.29 [0; 0 | $e+1$, $e+1$, $-e-1$, $e+1$, $-e-1$, $-e-1$] [1.5; 0 | $-e-1$, $e+1$, −15, 6]
charmed baryons (C = +1):	
Λ_C^+	2286.46 ±0.14 [1.5; 0 | $-e-1$, $-e-1$, 45, −15]
$\Lambda_C(2595)^+$	2595.4 ±0.6 [1.5; 0 | −6, 6, $e+1$, $-e-1$, ***]
$\Lambda_C(2625)^+$	2628.1 ±0.6 [1.5; 0 | −6, 12, 6]
$\Lambda_C(2880)^+$	2881.53 ±0.35 [1.5; 0 | −6, $-e-1$, $e+1$, ***]

Table 4: Continued fraction representation of particle masses according to equation (4).

Particle	Particle mass with standard deviation. Continued fraction representation
charmed baryons (C = +1):	
$\Sigma_C(2455)^{++}$	2454.02 ±0.18 [1.5; 0 | −6, $e+1$, $-e-1$, $e+1$, $e+1$, $-e-1$, $e+1$]
$\Sigma_C(2455)^+$	2452.9 ±0.4 [1.5; 0 | −6, $e+1$, $-e-1$, $e+1$, $e+1$]
$\Sigma_C(2455)^0$	2453.76 ±0.18 [1.5; 0 | −6, $e+1$, $-e-1$, $e+1$, $e+1$, $-e-1$]
Ξ_c^+	2467.8 ±0.6 [0; 0 | $e+1$, $-e-1$, $e+1$, 60] [1.5; 0 | −6, $e+1$, $-e-1$, −15]
Ξ_c^0	2470.88 ±0.8 [0; 0 | $e+1$, $-e-1$, $e+1$, −162] [1.5; 0 | −6, $e+1$, $-e-1$, −6]
$\Xi_c(2645)^+$	2645.9 ±0.6 [1.5; 0 | −6, 21, −6]
$\Xi_c(2645)^0$	2645.9 ±0.5 [1.5; 0 | −6, 21, −6]
$\Xi_c(2815)^+$	2816.6 ±0.9 [1.5; 0 | −6, $-e-1$, 12]
$\Xi_c(3080)^+$	3077.0 ±0.4 [1.5; 0 | −9, 9, 18]
light unflavored mesons (S = C = B = 0):	
$\pi^\pm$	139.57018 ±0.00035 [1.5; −3 | −6, $-e-1$, 18, $-e-1$, $e+1$, $-e-1$, $e+1$]
π^0	134.9766 ±0.0006 [1.5; −3 | −6, −15, $e+1$, $-e-1$, −33]
η	547.853 ±0.024 [0; 0 | −6, $e+1$, $-e-1$, 6, $-e-1$, 12] [1.5; −3 | $e+1$, $-e-1$, $e+1$, 9, $-e-1$, $-e-1$]
$\rho(770)$	775.49 ±0.34 [0; 0 | −15, $-e-1$]
$\omega(782)$	782.65 ±0.12 [0; 0 | −15]
$\rho'(958)$	957.78 ±0.06 [0; 0 | 132]
$\phi(1020)$	1019.455 ±0.02 [0; 0 | 33, −12, $e+1$]
$f_1(1285)$	1281.8 ±0.6 [0; 0 | 9, −9, −6]
$a_2(1320)$	1318.3 ±0.6 [0; 0 | 9, $-e-1$, $e+1$, $-e-1$, $e+1$, $-e-1$]
$f_1(1420)$	1426.4 ±0.9 [0; 0 | 6, 6, −6]
strange mesons (S =±1, C = B = 0):	
$K^\pm$	493.667 ±0.016 [0; 0 | $-e-1$, −6, $e+1$, 39]
K^0	497.614 ±0.024 [1.5; −3 | $e+1$, $-e-1$, $-e-1$, $e+1$, $-e-1$]

Particle	Particle mass with standard deviation. Continued fraction representation
strange mesons (S =±1, C = B = 0):	
$K^*(892)^{\pm}$	891.66 ±0.26 [0; 0 | −54, e+1]
$K^*(892)^0$	896.00 ±0.25 [0; 0 | −60, e+1]
charmed mesons (S =±1):	
$D^{\pm}$	1869.62 ±0.2 [0; 0 | e+1, 12, 24]
D^0	1864.84 ±0.17 [0; 0 | e+1, 12, −e−1, −e−1]
$D^*(2007)^0$	2006.97 ±0.19 [0; 0 | e+1, −18, −e−1, e+1, −e−1] [1.5; 0 | −e−1, 63]
$D^*(2010)^{\pm}$	2010.27 ±0.17 [0; 0 | e+1, −18, −216] [1.5; 0 | −e−1, 78]
charmed, strange mesons (C = S =±1):	
$D_s^{\pm}$	1968.49 ±0.34 [0; 0 | e+1, −54]
$D_s^{*\pm}$	2112.3 ±0.5 [1.5; 0 | −e−1, −12, 15]
$D_{S0}^*(2317)^{\pm}$	2317.8 ±0.6 [0; 0 | e+1, −e−1, −27] [1.5; 0 | −e−1, −e−1, 6, −e−1, −e−1]
$D_{S1}(2460)^{\pm}$	2459.6 ±0.6 [0; 0 | e+1, −e−1, e+1, 12] [1.5; 0 | −6, e+1, −e−1, 9]
$D_{S1}(2536)^{\pm}$	2535.35 ±0.34 [0; 0 | e+1, −e−1, e+1, −e−1, e+1, e+1] [1.5; 0 | −6, e+1, e+1, e+1]
$D_{S2}(2573)^{\pm}$	2572.6 ±0.9 [1.5; 0 | −6, 6, −15]
bottom mesons (B =±1):	
$B^{\pm}$	5279.17 ±0.29 [1.5; 0 | 12, −54]
B^0	5279.5 ±0.3 [1.5; 0 | 12, −51]
B^*	5325.1 ±0.5 [1.5; 0 | 12, −6, 6]
bottom, strange mesons (S = B =±1):	
B_S^0	5366.3 ±0.6 [1.5; 0 | 12, −e−1, 6, −e−1]
cc-mesons (S = B =±1):	
$J/\Psi(1S)$	3096.916 ±0.011 [1.5; 0 | −9, 24]
$X_{c0}(1P)$	3414.75 ±0.31 [1.5; 0 | 12, −e−1, e+1, ***]
$X_{c1}(1P)$	3510.66 ±0.07 [1.5; 0 | −15, −45]
$h_c(1P)$	3525.67 ±0.32 [1.5; 0 | −15, −6, −6]

Particle	Particle mass with standard deviation. Continued fraction representation
cc-mesons (S = B =±1):	
$X_{c2}(1P)$	3556.20 ±0.09 [1.5; 0 | −15, −e−1, e+1, ***]
$\Psi(2S)$	3686.09 ±0.04 [1.5; 0 | −21, 9, −e−1, e+1, ***]
$\Psi(3770)$	3772.92 ±0.35 [1.5; 0 | −24, −e−1, e+1, ***]
$X(3872)$	3872.3 ±0.8 [1.5; 0 | −33]
$Y(1S)$	9460.3 ±0.26 [0; 3 | −e−1, −12, −87]
$X_{b0}(1P)$	9859.44 ±0.42 [0; 3 | −e−1, −6, 9, −15] [1.5; 0 | e+1, −6, e+1, −6, e+1, −e−1]
$X_{b1}(1P)$	9892.78 ±0.26 [1.5; 0 | e+1, −6, e+1, −e−1, e+1, −9]
$X_{b2}(1P)$	9912.21 ±0.26 [0; 3 | −e−1, −6, e+1, 15, −e−1]
$Y(2S)$	10023.76 ±0.31 [0; 3 | −e−1, −e−1, −e−1, −e−1] [1.5; 0 | e+1, −e−1, −e−1, e+1, 12, −e−1]
$X_{b0}(2P)$	10232.5 ±0.4 [0; 3 | −e−1, −e−1, 327] [1.5; 0 | e+1, −e−1, −6, −e−1, e+1, −e−1]
$X_{b1}(2P)$	10255.46 ±0.22 [0; 3 | −e−1, −e−1, 30, 6]
$X_{b2}(2P)$	10268.65 ±0.22 [0; 3 | −e−1, −e−1, 21, −e−1] [1.5; 0 | e+1, −e−1, −9, 6, 6]
$Y(3S)$	10355.2 ±0.5 [0; 3 | −e−1, −e−1, 6, e+1, 6] [1.5; 0 | e+1, −e−1, −18, 9]
leptons:	
Electron	0.510998910 ±0.000000013 [1.5; −9 | −177]
μ	105.658367 ±0.000004 [0; −3 | e+1, −6, −e−1, e+1, ***]
τ	1776.84 ±0.17 [0; 0 | e+1, 6, −e−1, e+1, −e−1, −e−1]
gauge bosons:	
W	80398 ±25 [1.5; 3 | −54, −e−1, e+1]
Z	91187.6 ±2.1 [1.5; 3 | 36, −6, e+1]

fortunately, these simple graphs do not provide information to distinguish between stable and unstable particles. The repeatedly occurring mass gaps from $2e$ to $\frac{e}{16}$ strongly support the idea that masses in the micro-cosmos are not random and have a self-similar, fractal structure. However, we emphasize that this fractal behavior is only a statistical influence with low priority, since we know for instance that nature realizes with the chemical elements easily the whole logarithmic mass range from 0 to $2e$ without significant mass gaps. Also it should be noted that the logarithmic mass differences in Table 3 are always approximately multiples of the fractions of e. This means the fractal property provides only a signature of regularities, becoming visible only on the logarithmic number line.

Due to the fact that frequently mass distances occur which are close, but not exactly a fraction of e, we decided to modify Müller's continued fractions (given in equation(2)). Specifically we abandon the canonical form and change all partial numerators to Euler's number. Furthermore we follow results published by Müller in one of his patents [9] and introduce a phase shift p in equation (2). According to [9] the phase shift can only have the values 0 or ± 1.5. So we write

$$\ln \frac{particle\ mass}{proton\ mass} = p + S\ , \tag{3}$$

where S is the continued fraction

$$S = n_0 + \cfrac{e}{n_1 + \cfrac{e}{n_2 + \cfrac{e}{n_3 + \ldots}}}\ . \tag{4}$$

We abbreviate $p + S$ as $[p; n_0 \mid n_1, n_2, n_3, \ldots]$. Provided that our initial assumption is correct, and the particles are resonance states, their masses should be located in the maximum spectral density areas. Consequently we must require that the free link n_0 and the partial denominators n_i are integers divisible by 3. For convergence reason, we have to include $|e + 1|$ as allowed partial denominator. This means the free link n_0 is allowed to be $0, \pm 3, \pm 6, \pm 9 \ldots$ and all partial denominators n_i can take the values $e + 1, -e - 1, \pm 6, \pm 9, \pm 12 \ldots$ In order to test the model very critically for a more extended set of particles we followed Müller's article [3] and selected all elementary particles which have their masses determined with a standard deviation $\leqslant 1$ MeV/c^2 and included additionally the gauge bosons due to their special importance (78 particles altogether). For the calculation of the continued fractions we assumed first that the mass values were without any measurement error. This means, equation (3) does not hold and one ideally obtains a continued fraction with an infinite number of partial denominators. For practical reasons we determined only 18 partial denominators. Next we calculated repeatedly the particle mass from the continued fraction, every time considering one more partial denominator. As soon as the calculated mass value (on the linear scale) was in the interval "*mass* ± *standard deviation*", we stopped considering further denominators and gave the resulting fraction in Table 4. In special cases, where the particle mass is much more accurately determined than the proton mass (e.g. electron) the standard deviation was set to that of the proton.

It was found that the great majority of the particle masses could be expressed by a continued fraction, which means that they are localized in nodes or sub-nodes. Only 10 particles were found to be localized in a gap. In such a case the continued fraction turns into an alternating sequence of $-e-1$ and $e+1$ without any further significant approximation to the mass value. In Table 4, this sequence was then abbreviated by three stars. It should be noted that the particle mass calculated from such a fraction is still close to the experimental value, but has a difference from the experimental value higher than the standard deviation. For around 50% of the particles, it was required to set the phase shift to 1.5 in order to get the masses located in a node or sub-node. For 14 particles, their masses can even be located in sub-nodes for both phase shifts (0 and 1.5). If so, both continued fractions were indicated in Table 4. As can be seen, the continued fractions have seldom more than 5 partial denominators, they can be even shortened abandoning the standard deviation requirement and accepting a small percentage error on the logarithmic scale as it was done in Müller's article [2].

There are, however some general questions open. It is clear that the continued fraction analysis provides a new system to put the particles in groups regarding the length of the fraction (fractal layers), the phase shift, value of the free link and the value of the numerator. Which of these parameters have physical meaning and which ones are just mathematics?

Especially regarding the physical significance of the nominator, more research must be done. We believe that is not coincidence that most of the masses become localized in nodes or sub-nodes when calculating the fractal spectrum with nominator e, similar calculations have shown that the numerators 2 or the golden ratio do not work in this manner. This however, was here found empirically, to the best of our knowledge there is no way to calculate directly which nominator reproduces best the fractal distribution. It must still be done by trial and error combined with intuition. Anyway, we suggest to abandon the canonical form of the continued fractions whenever possible, since with numerator 1, actually some physical information of the fractal distribution is lost. It is known that continued fractions with arbitrary numerator $\neq 1$ can be transformed into fractions with numerator equal to 1, via Euler equivalent transformation.

From the presented numerical results, some ideas can be derived:

1. The three most stable here considered particles are the electron, proton and neutron with half-life of around 11 minutes. Their continued fraction representations are quite short, consisting only of the free link and one

partial denominator. Possibly short continued fractions indicate stability. Furthermore the very high values of the first partial denominators n_1 indicate two facts: a proximity to the node n_0 and an irrelevance of any further partial denominator which can change the value of the fraction only insignificantly. This means a high value of n_1 might also be considered as a criterion for stability.

2. According to reference [1], in a node, there is a change from spectral compression to spectral decompression, which means that with a certain probability a change in process trend can be observed. This statement is in agreement with the continued fraction representations of the electron and the neutron. The electron [1.5; −9 | −177] lies with a negative first partial denominator closely before the principal node [1.5; −9], whereas the neutron [0; 0 | 1973] is positioned right after the principal node [0; 0] due to its positive denominator. This means the electron in the compression range is stable whereas the neutron is in a decompression range and already exhibits decay property.

4 Resume

Numerical investigation of particle masses revealed that 87% of the considered elementary particles can be interpreted as proton resonance states. We cannot expect that all particle masses are only governed by proton resonance properties, other natural laws apply as well. The here presented mathematical model can be modified in various ways and future research should concentrate on identifying fractal properties in other data sets such as half-lifes of radioactive nuclides or mass defects, utilizing either our or similarly modified continued fractions. Only when multiple fractal data sets are known, the possible numerical values of the numerator or the phase shift can be adequately interpreted and maybe attributed to a physical property.

Acknowledgements

The authors greatly acknowledge the financial support from the Brazilian governmental funding agencies FAPESQ and CNPq.

Submitted on July 21, 2010 / Accepted on August 11, 2010

References

1. Müller H. Fractal scaling Models of resonant oscillations in chain systems of harmonic oscillators. *Progress in Physics*, 2009, v. 2, 72–76.
2. Müller H. Fractal scaling models of natural oscillations in chain systems and the mass distribution of the celestial bodies in the solar system. *Progress in Physics*, 2010, v. 1, 62–66.
3. Müller H. Fractal scaling models of natural oscillations in chain systems and the mass distribution of particles. *Progress in Physics*, 2010, v. 3, 61–66.
4. Anders E., Grevesse N. Abundances of the elements — meteoritic and solar. *Geochimica et Cosmochimica Acta*, 1989, v. 53, 197–214.
5. Audi G., Wapstra A. H., Thibault C. The AME2003 atomic mass evaluation (II). Tables, graphs and references. *Nuclear Physics A*, 2003, v. 729, 337–676.
6. Lide D. R. (Editor) CRC Handbook of Chemistry and Physics. CRC Press, Boca Raton, 2005.
7. Press W. H., Teukolsky S. A., Vetterling W. T., Flannery B. P. Numerical recipes in C. Cambridge University Press, Cambridge, 1992.
8. Bethe H. A. Energy production in stars. *Physical Review*, 1939, v. 55, 434–456.
9. Otte R., Müller H. German patent No. DE102004003753A1, date: 11.08.2005.